



Defence Research and
Development Canada

Recherche et développement
pour la défense Canada



Synthesis of nonlinear guidance laws for missiles with uncertain dynamics

C. A. Rabbath
DRDC Valcartier

N. Lechevin
NSERC Visiting Fellow (DRDC Valcartier)

Defence R&D Canada – Valcartier

Technical Memorandum

DRDC Valcartier TM 2006-606

November 2007

Canada

Synthesis of nonlinear guidance laws for missiles with uncertain dynamics

C.A. Rabbath
DRDC Valcartier

N. Lechevin
NSERC Visiting Fellow (DRDC Valcartier)

Defence Research and Development Canada - Valcartier

Technical Memorandum

DRDC Valcartier TM 2006-606

November 2007

Author

C.A. Rabbath, N. Lechevin

Approved by

A. Jouan, Head, Precision Weapons Section

Approved for release by

C. Carrier, Chief Scientist, DRDC Valcartier

This work was carried out under WBE 13ef11 between January 2004 and March 2005.

© Her Majesty the Queen as represented by the Minister of National Defence, 2007

© Sa majesté la reine, représentée par le ministre de la Défense nationale, 2007

Abstract

This technical memorandum describes a nonlinear guidance law for a single-missile single-target engagement. The guidance relies on the concepts of Lyapunov stability and backstepping, which are constructive methods in nonlinear control theory. The design of the guidance law allows taking into account the nonlinear relative kinematics between the missile and the target, and ensuring ultimate boundedness of the missile-target system trajectories provided the estimation error of the target acceleration is bounded in magnitude. In other words, despite the nonlinear kinematics between the missile and the target, the guidance scheme is guaranteed to result in a relatively small miss distance between the missile and the target.

There are two steps in designing the nonlinear guidance law. In the first step, using the fully nonlinear missile-target engagement kinematics, an appropriate Lyapunov function candidate is selected and a state-feedback law is obtained. Closed-loop pole placement using linear matrix inequalities provides an ultimate bound to the maximum allowable miss distance, assuming idealized flight control dynamics; that is, infinitely fast reaction times for the missile. In the second step of the guidance law, the control law is robustified by means of a high-gain backstepping approach, taking into account the uncertain flight control dynamics of the pursuer missile as an uncertain although bounded time constant. Numerical simulations of the nonlinear guidance in closed-loop with a missile modeled as an interval second-order transfer function and a maneuvering target demonstrate satisfactory performances when compared to modern and classical guidance laws, such as proportional navigation guidance. Despite the uncertainty on the missile flight control system, which is usually the case in practice, the guidance law achieves small miss distances against highly maneuverable targets. Uncertainties may arise due to a variety of reasons. For instance, uncertainties may be due to variations in the missile aerodynamics over the flight envelope, unexactly known aerodynamic performance, or low-order approximate modeling of the flight control system. However, it is important to note that the satisfactory performance of the nonlinear guidance comes at the expense of potentially large acceleration demands in the early part of the terminal phase of the engagement, when the guidance law is applied. There is therefore a trade-off to be made between the reduction of the miss distance and the acceleration demands.

Résumé

Ce mémorandum technique présente une loi de guidage non linéaire pour un engagement un contre un. La méthode de guidage repose sur les concepts de stabilité de Lyapunov et de rétrogradation (*backstepping*). Ces dernières sont des méthodes constructives dans le domaine de la commande non linéaire. La conception de la loi de guidage permet de prendre en compte la cinématique non linéaire entre le missile et la cible, et assure une borne ultime des trajectoires du système missile-cible dans la mesure où l'erreur d'estimation de l'accélération de la cible soit bornée en amplitude. Autrement dit, malgré la cinématique non linéaire entre le missile et la cible, la méthode de guidage présentée garantit une erreur de passage relativement petite entre le missile et la cible.

La conception du guidage non linéaire se fait en deux étapes. Premièrement, une fonction de Lyapunov est sélectionnée et une loi de rétroaction par état est obtenue en tenant compte de la cinématique non linéaire entre le missile et la cible. Un placement de pôles utilisant les matrices d'inégalités linéaires permet d'obtenir une borne ultime à l'erreur de passage, en supposant une dynamique de commande de vol idéale. Deuxièmement, la loi de commande est rendue robuste au moyen de l'approche *backstepping* tout en prenant en compte la dynamique incertaine de la commande de vol sous la forme d'une constante de temps incertaine. Des simulations numériques du guidage non linéaire en boucle fermée avec le système de commande de vol du missile, qui est modélisé comme une fonction de transfert de deuxième ordre à intervalles, et d'une cible manoeuvrante démontrent les performances obtenues avec la méthode proposée en comparaison avec des méthodes dites modernes et traditionnelles de guidage telles que la navigation proportionnelle. Malgré l'incertitude de la commande de vol du missile, qui est généralement présente en pratique, le guidage non linéaire résulte en de petites erreurs de passage contre des cibles hautement manoeuvrables. Cependant, il est important de noter que la performance du guidage non linéaire a un coût. Il est possible que de larges accélérations soient nécessaires dans la partie initiale de la phase terminale de l'engagement. Donc, il y a un compromis à faire entre réduire l'erreur de passage et obtenir des accélérations acceptables.

Executive Summary

Guidance is a key component of any missile. To achieve intercept, it is crucial that the software provide appropriate control actions to strike maneuvering targets. In this context, this technical memorandum presents a nonlinear guidance law for single-missile, single-target engagement. The design of the guidance law relies on nonlinear control theory, which is required in typical missile-target engagement as the kinematics between the two vehicles are highly nonlinear. The design of the guidance law allows taking into account the nonlinear relative kinematics between the missile and the target, and ensuring ultimate boundedness of the missile-target system trajectories provided the estimation error of the target acceleration is bounded in magnitude. The estimation of the acceleration of the target is not explicitly detailed in this memorandum, and would possibly rely on a target state estimation algorithm. Despite the nonlinear kinematics between the missile and the target, the guidance scheme guarantees the achievement of a relatively small miss distance.

Despite the uncertainty on the missile flight control system, which is usually the case in practice, the guidance law achieves small miss distances against highly maneuverable targets. Simulation results showed a reduction of the miss distance, in the case of highly maneuverable targets, up to a ratio of 5:1 when using the proposed guidance law over other proportional navigation guidance (PNG)-based techniques. PNG and its variants have been extensively studied and used because of their computational simplicity and optimal performance in the pursuit of non-maneuvering targets. However, as is well known, PNG may become ineffective for the interception of highly maneuvering targets for which nonlinearities of the missile-target configurations are predominant. However, it is important to note that the satisfactory performance of the proposed nonlinear guidance law comes at the expense of potentially large acceleration demands in the early part of the terminal phase of the engagement, when the guidance law is applied. This trade-off between reduction of miss distance and amplitude of missile accelerations must be appropriately handled by the designer.

The guidance law has the potential to impact on military practice by providing increased probabilities of intercepts despite imprecise knowledge of the aerodynamics of the pursuer missile, imperfect target information, and relatively high maneuvers of target, a capability that is not offered with currently used guidance laws, such as the classical PNG.

Sommaire

Le guidage est une composante clé de tout missile. Pour réussir l'interception, il est crucial que le logiciel à bord du missile génère les actions de commande appropriées pour frapper des cibles toujours plus manoeuvrables. Dans ce contexte, ce mémorandum technique présente une loi de guidage non linéaire pour un engagement un contre un. La conception de la loi de guidage repose sur la théorie de la commande non linéaire, qui est requise dans ce genre d'engagements, puisque la cinématique entre le missile et la cible est hautement non linéaire. Entre autres, les concepts de stabilité de Lyapunov et de *backstepping* sont utilisés pour développer la loi de guidage non linéaire. Le *backstepping* est une méthode constructive dans la théorie de la commande non linéaire qui permet de stabiliser le missile autour de son point d'équilibre; c'est-à-dire lorsque le missile est dans un triangle de collision avec la cible. La conception de la loi de guidage permet de prendre en compte la cinématique non linéaire entre le missile et la cible, et d'assurer une borne ultime des trajectoires du système missile-cible en autant que l'erreur d'estimation de l'accélération de la cible soit bornée en amplitude. La façon d'obtenir l'estimation de l'accélération de la cible n'est pas décrite dans ce mémorandum.

Malgré la cinématique non linéaire entre le missile et la cible, la méthode de guidage non linéaire garantit une erreur de passage relativement petite. La conception du guidage non linéaire se fait en deux étapes. Premièrement, une fonction de Lyapunov est sélectionnée et une loi de rétroaction par état est obtenue en tenant compte de la cinématique non linéaire entre le missile et la cible. Un placement de pôles utilisant les matrices d'inégalités linéaires permet d'obtenir une borne ultime à l'erreur de passage, en supposant une dynamique de commande de vol idéale. Deuxièmement, la loi de commande est rendue robuste par l'approche *backstepping* tout en prenant en compte la dynamique incertaine de la commande de vol sous la forme d'une constante de temps incertaine. Des simulations numériques du guidage non linéaire en boucle fermée avec le système de commande de vol du missile, qui est modélisé comme une fonction de transfert de deuxième ordre à intervalles, et d'une cible manoeuvrante démontrent les performances obtenues avec la méthode proposée en comparaison avec des méthodes dites modernes et traditionnelles de guidage telles que la navigation proportionnelle. Malgré l'incertitude sur la commande de vol du missile, qui est généralement présente en pratique, le guidage non linéaire résulte en de petites erreurs de passage contre des cibles hautement manoeuvrables. Cependant, il est important de noter que la performance du guidage non linéaire a un coût. Il est possible que de larges accélérations soient nécessaires dans la partie initiale de la phase terminale de l'engagement. Donc, il y a un compromis à faire entre réduire l'erreur de passage et obtenir des accélérations acceptables.

La loi de guidage offre un potentiel certain pour influencer les pratiques militaires en augmentant les probabilités d'interception malgré une connaissance imprécise de l'aérodynamique du missile poursuivant, une information imparfaite provenant

de la cible, et des manoeuvres importantes de la cible, une capacité qui est inexistante avec des lois de guidage telles que la loi de navigation proportionnelle.

Table of Contents

Abstract.....	i
Résumé.....	ii
Executive Summary	iii
Sommaire.....	iv
Table of Contents.....	vi
List of Figures.....	vii
1. Introduction.....	1
2. Modeling of engagement kinematics and dynamics.....	4
2.1 Missile Flight Control System.....	4
2.2 Kinematics.....	5
2.3 Assumptions and definitions.....	7
3. Nonlinear homing guidance laws.....	10
3.1 Step 1: Synthesis of guidance law for idealized dynamics.....	11
3.2 Step 2: Guidance synthesis considering uncertain missile dynamics.....	13
4. Numerical simulations.....	18
4.1 Numerical models and guidance laws.....	18
4.2 Maneuvering target.....	20
5. Concluding remarks.....	27
6. References.....	28
List of symbols/abbreviations/acronyms/initialisms	31
Distribution List.....	32

List of Figures

Figure 1: Missile guidance and control.....	4
Figure 2: Engagement geometry - collision triangle.....	5
Figure 3: Structure of nonlinear guidance.....	10
Figure 4: Missile-target trajectories.....	16
Figure 5: Block diagram of missile control system.....	18
Figure 6: Influence of missile dynamics on miss distance.....	20
Figure 7: (a) Mean values $E(y(t_f))$ for the absolute miss distances with $a_t^{\max} = 10g$, and $\omega_t = 1.7$ rad/s; (b) zoom in over $[0 \text{ m}; 0.5 \text{ m}]$	22
Figure 8: (a) Standard deviations $\sigma_{y(t_f)}$ on the miss distances with $a_t^{\max} = 10g$, and $\omega_t = 1.7$ rad/s; (b) zoom in over $[0 \text{ m}; 0.1 \text{ m}]$	22
Figure 9: Absolute value of miss distance for different values of ω_t with $t_f = 5$, $a_t^{\max} = 10 \text{ g}$ and nominal parameters $\bar{\omega}$ and $\bar{\xi}$	23
Figure 10: (a) Absolute value of miss distance for different values of a_t^{\max} (g) with $t_f = 5$, $\omega_t = 1.7$ rad/s and nominal parameters $\bar{\omega}$ and $\bar{\xi}$; (b) zoom in over $[0 \text{ m}, 3 \text{ m}]$	24
Figure 11: Mean value of the energy consumed by the missile $E\left(\int_0^t a_m^2(\tau) d\tau\right)$ with $\omega_t = 1.7$ rad/s and $a_t^{\max} = 10g$	25
Figure 12: Comparison of actual missile accelerations with $\omega_t = 1.7$ rad/s, $a_t^{\max} = 10 \text{ g}$ and nominal parameters $\bar{\omega}$ and $\bar{\xi}$	26

This page intentionally left blank

1. Introduction

Proportional navigation guidance (PNG) [1] and its variants [2] have been extensively studied and used because of their computational simplicity and optimal performance in the pursuit of non-maneuvering targets [3]. However, as is well known, PNG may become ineffective for the interception of highly maneuvering targets for which nonlinearities of the missile-target configurations are predominant [4].

Several nonlinear guidance laws have been proposed to tackle such guidance problems. For example, [5] derived a command-line-of-sight guidance for surface-to-air missiles using feedback linearization. [6] presented a guidance strategy characterized by a switching between a feedback linearizing guidance, when the missile is far from the intercept triangle, and PNG, when the missile is in the vicinity of the collision course. The guidance law proposed in [6] is effective for a wide range of headings; however, the guidance does not take into account flight dynamics and the inherent uncertainties. [7] proposed a variable structure nonlinear guidance and autopilot considering zero-effort miss. [8] used differential geometry curve theory for the design of a guidance system for a class of target behaviors. [9] proposed improving PNG by using the Lyapunov method on the nonlinear missile-target system. The Lyapunov function candidate proposed in [9] is the square of the line-of-sight (LOS) derivative and is valid for both small-angle approximations to the missile-target kinematics and full nonlinear kinematics, although ideal flight control dynamics are assumed. [10] presents a nonlinear guidance using Lyapunov optimizing feedback control, where a descent function is selected and a feedback control is chosen, based on steepest and quickest descents, such that the descent function decreases at every state of the nonlinear missile-target system. Given mild conditions, asymptotic stability of the missile-target system can be achieved with the approach proposed in [10]. It was shown that such control law provides satisfactory performance against maneuvering targets, and in the presence of measurement noise and flight control dynamics expressed as time delay in the guidance loop. Circular navigation guidance proposed in [11] is based on the idea of circular arc following, theoretically warranting zero miss distance and desired impact angle provided reasonable conditions are satisfied, although target maneuvers are not considered in the synthesis.

It is clear that most novel nonlinear guidance synthesis and closed-loop analyses consider ideal missile dynamics, although it is known that the missile flight control constrains the performance achievable with the guidance loop [12]. For instance, there is an inherent time constant associated with the missile flight control in response to guidance commands, the actuator have their own dynamic characteristics, and the missile under closed-loop control exhibits a varying dynamical behavior throughout the flight envelope. Therefore, devising guidance laws on the premise that the missile will react instantaneously to the commanded accelerations is a limited, unrealistic approach. In this context, the work in [13]

proposed an integrated robust guidance and autopilot law, which comprises a zero-effort-miss guidance and a neural-network-based adaptive backstepping controller. The integrated guidance and control scheme proposed in [13] compensates for the error dynamics due to the pursuer missile modelling uncertainties and is shown to result in small miss distances and robust aerodynamic responses. Recently, [14] proposed an adaptive nonlinear guidance law using sliding mode control, where uncertainties in the target acceleration and in the dynamics of the flight control of the pursuer missile are taken into account by means of parameter adaptation. In [14], the guidance and the flight control loops are integrated in the model of the missile-target system. Nonlinearities of the kinematics are taken into account in the guidance synthesis, although trigonometric functions are approximated by assuming small angles. The flight control dynamics are modelled as a second order state-space model to which is added an exogenous disturbance representing approximation errors due to the use of curve fitting techniques in the modelling of aerodynamic parameters; however, it is unclear how the uncertainties impact the missile time constant, which can substantially fluctuate throughout the flight envelope.

In this technical memorandum, a Lyapunov-based nonlinear homing guidance law is presented. The guidance synthesis takes into account both the algebraic nonlinearities involved in the missile-target kinematics and the uncertain flight control dynamics. There is no simplification in the form of small angle approximation. Intuitively, considering the full nonlinear kinematics involved in missile-target engagements is expected to improve the performance of the pursuer missile, i.e. to provide small miss distances despite maneuvers of the target. Furthermore, considering uncertainties involved with the missile flight control system in the guidance synthesis is expected to warrant intercept despite the lack of perfect information on the missile's aerodynamics and on the target state. The imperfect information on the target state can be assumed to occur due to seeker inaccuracies. In this technical memorandum, flight control dynamics are modeled as a low-order system with an uncertain, time-varying time constant. The proposed guidance synthesis is divided into two steps. In the first step, a state-feedback law is obtained with the selection of an appropriate Lyapunov function candidate. The state is such that it comprises information of both pursuer missile and target. A Linear Matrix Inequality (LMI) [15], [16] pole characterization provides an ultimate bound to the maximum allowable miss distance assuming the flight control dynamics are ideal and the error in the estimate of the target acceleration is bounded. In the second step, the control law is robustified by means of a high-gain backstepping approach. Thus, even without perfect information on the missile flight control dynamics, the guidance scheme is guaranteed to provide satisfactory performance. As is well known, differentiating signals in real-time is to be avoided due to noise amplification. Thus, a high-gain approach, which avoids the need for computing derivatives, is used to dominate the uncertainty represented by the time constant [17]. Numerical simulations of the proposed guidance in closed-loop with an interval second-order missile transfer function and a maneuvering target demonstrate

superior performances than those obtained with modern and classical guidance laws despite uncertainties in the flight control system and high maneuverability of the target. Furthermore, it is shown that using target acceleration estimates in the guidance law results in relatively small miss distance even when the pursuer-evader maneuverability ratio [18] approaches unity. The latter case is particularly difficult to handle with classical guidance schemes such as PNG.

The technical memorandum is organized as follows. Chapter 2 provides the model of the engagement and the assumptions. The nonlinear guidance law is described in Chapter 3. Numerical simulations of a missile pursuing a maneuvering target with a sinusoidal-type normal acceleration with constant amplitude and pulsation are given in Chapter 4. Finally, the concluding remarks are presented in Chapter 5.

2. Modeling of engagement kinematics and dynamics

2.1 Missile Flight Control System

The system that drives the missile to the required accelerations is the so-called missile flight control system. Actuators may be DC and torque motors whereas sensors are typically rate gyros and accelerometers. Flight control systems are designed for roll control and for lateral and longitudinal acceleration tracking, where the acceleration commands are issued by the guidance system [12]. It is assumed that the flight control system is well designed for all of the operating points; that is, the control system provides satisfactory acceleration tracking and rate stabilization. Schematics of the flight control and guidance systems are shown in Figure 1. In the figure, the direction of the information flow is represented by the arrows.

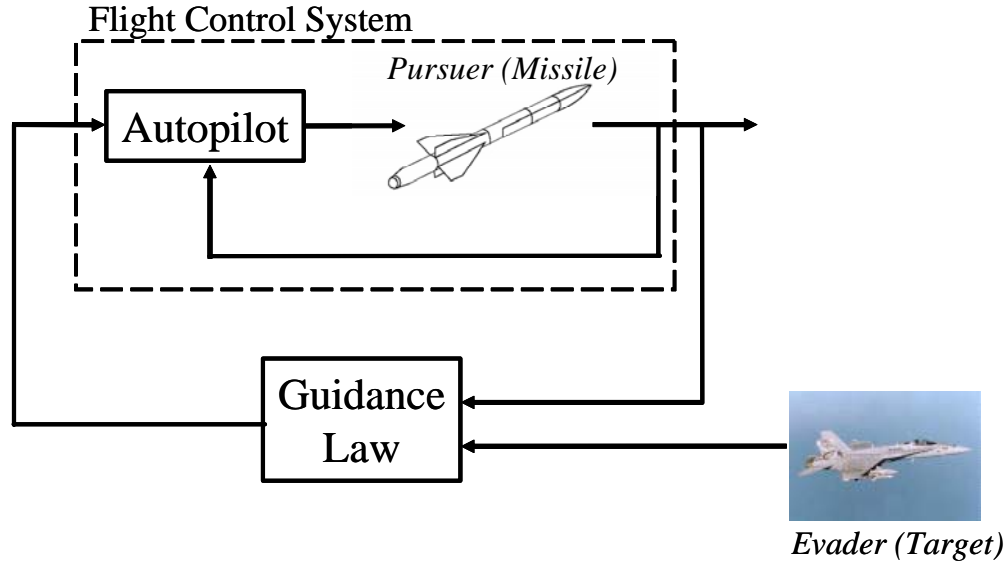


Figure 1: Missile guidance and control

Flight control system dynamics approximated as a first-order linear uncertain system allows to incorporate variations of some of the key parameters over the flight envelope while providing tractability in the guidance problem. Such approximation is not new and has been done in works such as [19]. Here, the flight control system dynamics are from the commanded acceleration to the actual missile acceleration normal to line-of-sight. Flight control system therefore corresponds to the missile in closed-loop with autopilot, as shown in Figure 1. Consider the first-order dynamics for a missile flight control system given as

$$\tau_1(t) \frac{dn_m(t)}{dt} = -n_m(t) + a_g(t) \quad (1)$$

where n_m is missile acceleration normal to the line-of-sight, a_g is commanded

acceleration, and the time constant of the flight control system is such that

$$\begin{aligned} 0 &< \underline{\tau}_1 \leq \tau_1(t) \leq \overline{\tau}_1, \\ 0 &< \underline{\tau}_1^d \leq \left| \frac{d\tau_1(t)}{dt} \right| \leq \overline{\tau}_1^d. \end{aligned}$$

The autopilot is assumed to have been designed such that parameter $\tau_1(t)$ has a finite upper bound $\overline{\tau}_1^d$. The lower ($\underline{\tau}_1 > 0$) and upper ($0 < \underline{\tau}_1 < \overline{\tau}_1$) bounds on the time constant can be determined from the behavior of the missile over the flight envelope of interest. Clearly, the missile flight control system will be behaving within these bounds as the aerodynamics are usually not perfectly known. The model given by (1) is assumed to preserve the overall time response characteristics of the actual missile flight control system. It should be noted that (1) with bounds $\underline{\tau}_1$ and $\overline{\tau}_1$ can be obtained by performing order reduction on a high-fidelity model of the missile flight control system dynamics by means of well established techniques such as balanced truncation [20].

2.2 Kinematics

The three-dimensional engagement of a missile for the intercept of a target is relatively complex. A more tractable two-dimensional engagement can be studied by assuming that the lateral and longitudinal planes are decoupled, as typically achieved through roll control [19]. The two-dimensional missile-target engagement geometry is shown in Figure 2, where v_m is missile speed, and v_t and n_t are the target speed and the target normal acceleration, respectively.

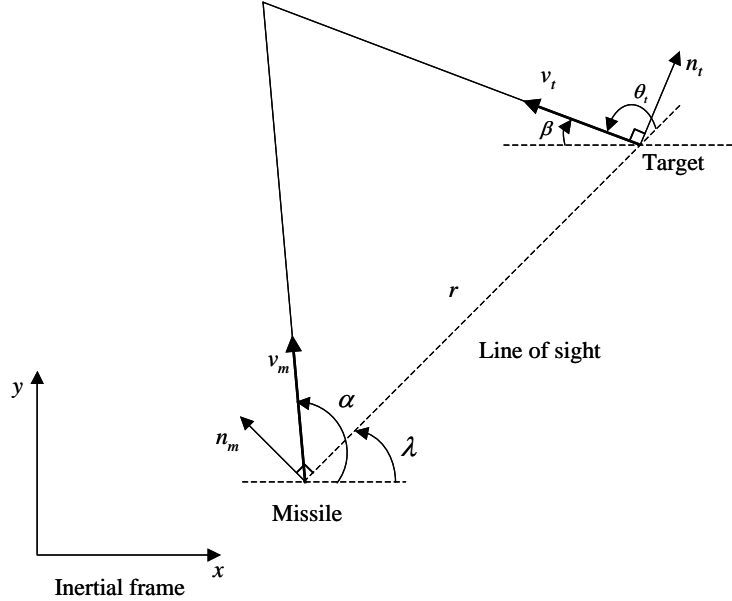


Figure 2: Engagement geometry - Collision triangle

The range r between the missile and the target is related to the closing velocity v_{cl} as follows

$$v_{cl}(t) = -\frac{dr(t)}{dt}. \quad (2)$$

The LOS angle $\lambda(t) \in]-\pi/2; \pi/2[$ is the angle between the LOS and the fixed reference. The sine of the LOS angle is given by $y(t)$, which is the relative separation between the missile and the target perpendicular to the fixed reference x -axis, over the range $r(t)$; that is,

$$\sin \lambda(t) = \frac{y(t)}{r(t)}. \quad (3)$$

From now on, reference to the independent time variable t is omitted unless stated otherwise. To obtain the state-space model for the missile-target kinematics, (3) is differentiated with respect to time. This yields

$$\frac{d\lambda}{dt} \cos \lambda = \frac{\frac{dy}{dt}r - y\frac{dr}{dt}}{r^2}. \quad (4)$$

Then, taking time derivative of (4), results in

$$\frac{d^2\lambda}{dt^2} \cos \lambda - \left(\frac{d\lambda}{dt}\right)^2 \sin \lambda = \frac{1}{r} \frac{d^2y}{dt^2} - 2\frac{d\lambda}{dt} \frac{dr}{dt} \cos \lambda - \frac{1}{r} \frac{d^2r}{dt^2} \sin \lambda \quad (5)$$

where the relative acceleration, d^2y/dt^2 , can be expressed as

$$\frac{d^2y}{dt^2} = a_t - a_m = n_t \cos \beta - n_m \cos \lambda. \quad (6)$$

For the missile-target kinematics, the following state variables are defined

$$x_1 = \sin \lambda - \sin \lambda_o, \quad (7)$$

$$x_2 = \frac{dx_1}{dt}, \quad (8)$$

where λ_o represents a fixed LOS angle at equilibrium. Angle λ_o can be interpreted as a desired kinematic constraint imposed on the missile-target behavior until intercept. Then,

$$\frac{dx_1}{dt} = \frac{d\lambda}{dt} \cos \lambda, \quad \frac{dx_2}{dt} = \frac{d^2\lambda}{dt^2} \cos \lambda - \left(\frac{d\lambda}{dt}\right)^2 \sin \lambda. \quad (9)$$

The missile-target kinematics given above can be formulated alternatively with the following state-space form

$$\begin{bmatrix} \frac{dx_1}{dt} \\ \frac{dx_2}{dt} \end{bmatrix} = Ax + Bf\left(r, \frac{dr}{dt}, \frac{d^2r}{dt^2}, \lambda, \frac{d\lambda}{dt}, a_t, a_m\right) \quad (10)$$

$$x_1(t_0) = \sin \lambda(t_0) - \sin \lambda_0 \quad (11)$$

$$x_2(t_0) = \frac{d\lambda}{dt}(t_0) \cos \lambda(t_0) \quad (12)$$

where t_0 is initial time (defined as zero in this memorandum),

$$A = \begin{bmatrix} 0 & 1 \\ 0 & 0 \end{bmatrix}, B = \begin{bmatrix} 0 \\ 1 \end{bmatrix}, x = \begin{bmatrix} x_1 \\ x_2 \end{bmatrix}, \quad (13)$$

and

$$\begin{aligned} f\left(r, \frac{dr}{dt}, \frac{d^2r}{dt^2}, \lambda, \frac{d\lambda}{dt}, a_t, a_m\right) &= -\frac{a_m}{r} + g\left(r, \frac{dr}{dt}, \frac{d^2r}{dt^2}, \lambda, \frac{d\lambda}{dt}, a_t\right) \\ g\left(r, \frac{dr}{dt}, \frac{d^2r}{dt^2}, \lambda, \frac{d\lambda}{dt}, a_t\right) &= \frac{a_t}{r} - \frac{2}{r} \frac{d\lambda}{dt} \frac{dr}{dt} \cos \lambda - \frac{1}{r} \frac{d^2r}{dt^2} \sin \lambda. \end{aligned} \quad (14)$$

Such equations correspond to the engagement geometry of Fig. 2.

2.3 Assumptions and definitions

Assumption 1 (Measurements) Even though measurements are often corrupted by noise, the present work is confined to deterministic signals exempt from noise. Furthermore, sensor dynamics are assumed to be significantly faster than missile-target dynamics so that they can be omitted.

Assumption 2 (Target Behavior) (a) The behavior considered is a maneuvering target with estimates $\hat{a}_t(t)$ available to the guidance law as delayed target accelerations, i.e. $\hat{a}_t(t) = a_t(t - \tau)$, where $\tau \in \mathcal{R}^+$. Note that \mathcal{R}^+ represents the set of positive real numbers, and \mathcal{R} is the set of real numbers. With the target acceleration being bounded as $|a_t(t)| < \frac{\overline{a}_t}{2}$, where upper bound $\overline{a}_t \in \mathcal{R}$, then $|\hat{a}_t(t) - a_t(t)| < \overline{a}_t$. (b) The target jerk is bounded, i.e. $|da_t/dt| < j_t \in \mathcal{R}^+$.

Target estimates may be obtained by means of on-board processing. Hence, *Assumption 2* provides a realistic limitation taken into account in the guidance synthesis.

Assumption 3 (Missile-Target Range) The range r between the missile and the target, and the first two time derivatives of the range are bounded as follows

$$r_m < r < r_M, \quad r_m, r_M \in \mathcal{R}, \quad (15)$$

$$\left| \frac{dr}{dt} \right| < r_M^v \in \mathcal{R}, \quad (16)$$

$$\left| \frac{d^2 r}{dt^2} \right| < r_M^a \in \mathcal{R}. \quad (17)$$

$$\left| \frac{d^3 r}{dt^3} \right| < r_M^j \in \mathcal{R}. \quad (18)$$

The first inequality in (15) is required to avoid singularities at intercept when the range becomes relatively small, and to confine the range to a maximum value. In general, a reasonable assumption is to define the smallest achievable miss distance r_m to be equal to half of the largest target dimension [21]. The second and third inequalities in (15) relate to limitations in velocities and accelerations of both the missile and the target. Obviously, missile and target maneuverability are constrained by their aerodynamics.

Definition 1 (Ultimately Bounded Trajectories) [22] Considering a nonlinear system given as

$$dx/dt = f(x), \quad (19)$$

where $f : [0, \infty) \times D \rightarrow R^n$ is piecewise continuous in t and locally Lipschitz in x on $[0, \infty) \times D$ and D is a subset of R^n that contains the origin. The evolution of the state x , or equivalently the trajectories, is said to be ultimately bounded with ultimate bound b if there exists positive constants b and c , independent of initial time $t_0 \geq 0$, and for every $a \in (0, c)$, there is a $T(a, b) \geq 0$ independent of t_0 such that

$$\|x(t_0)\| \leq a \implies \|x(t)\| \leq b \quad (20)$$

for all $t \geq t_0 + T$.

Systems satisfying *Definition 1* have their trajectories approaching a known region in the state space. Over time, the state trajectories will enter a ball with a certain radius. If the guidance can be designed such that the missile-target states, consisting of LOS angle and LOS rate, satisfy *Definition 1*, despite the uncertain dynamics of the missile, then it is expected that the missile performance will be improved when compared to classical guidance which does not warrant ultimate boundedness for the nonlinear engagement. In other words, with careful synthesis of the guidance scheme, the LOS rate can be made arbitrarily close to zero, and hence miss distance is expected to be small based on the collision triangle. The designer, however, has to be careful with the magnitude of the resulting acceleration demands.

Definition 2 (Asymptotic stability)[22] Let $x^* = 0$ be an equilibrium point for a nonlinear system $dx/dt = f(x)$ and $D \subset R^n$ be a domain containing x^* . Let $V : D \rightarrow R$ be a continuously differentiable function such that

$$V(0) = 0 \text{ and } V(x) > 0 \text{ in } D - \{0\}$$

$$dV(x)/dt < 0 \text{ in } D$$

Then, x^* is asymptotically stable. The function V , called the Lyapunov function, decreases along the trajectory x . Note: as $t \rightarrow \infty$, $x \rightarrow x^*$.

3. Nonlinear homing guidance laws

In this section, the nonlinear homing guidance laws, with a general structure as shown in Figure 3, are presented. In the figure, the hat denotes an estimated variable. Two laws are proposed. One is labeled as nonlinear PNG (NLPNG), whereas the other is denoted as nonlinear PNG with target acceleration (NLPNG+ a_t). The latter uses the target acceleration estimate whereas the former does not.

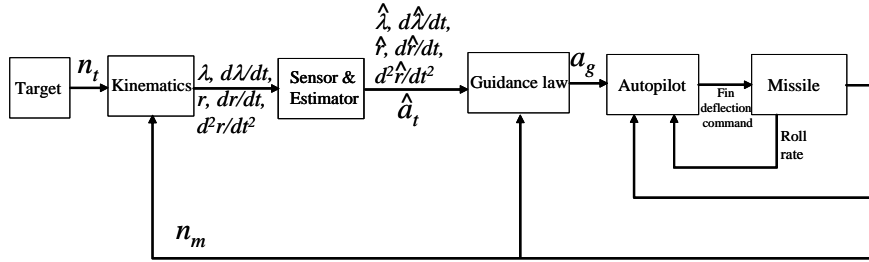


Figure 3: Structure of nonlinear guidance

As stated in [1], if system lags, such as those of the missile body dynamics, the autopilot and the seeker, are unaccounted for by the guidance law, there can potentially result large miss distances. Furthermore, it is well known that ignoring target maneuvers in the design of a guidance law may yield relatively large miss distances. In this memorandum, guidance laws taking into account system lags and target maneuver are proposed. A two-step high-gain backstepping procedure [17] is presented. First, a design based on idealized missile dynamics is carried out. Then, the uncertain dynamics are introduced to finalize the guidance law. The lag associated with the response time of the missile flight control is taken into account in the second step of the guidance synthesis. Such two-step approach leads to the following missile guidance law:

$$a_g = (k + k_\tau - \frac{\overline{\tau_1}}{2} k_{vs} \frac{d\lambda}{dt} \tan \lambda) (\mu_g - n_m) + n_m + x^T \frac{PB}{r}, \quad (21)$$

$$k > 0, k_\tau \geq \frac{\overline{\tau_1 d}}{2} \quad (22)$$

$$k_{vs} = \begin{cases} 0 & \text{if } \frac{d\lambda}{dt} \sin \lambda \geq 0 \\ 1 & \text{if } \frac{d\lambda}{dt} \sin \lambda < 0 \end{cases} \quad (23)$$

with

$$\begin{aligned} \mu_g &= N v_{cl} \frac{d\lambda}{dt} + g^* \left(r, \frac{dr}{dt}, \frac{d^2r}{dt^2}, \lambda, \frac{d\lambda}{dt}, \hat{a}_t \right) - \frac{r}{\cos \lambda} K \begin{bmatrix} x_1 \\ x_2 \end{bmatrix} \\ g^* \left(\frac{dr}{dt}, \frac{d^2r}{dt^2}, \lambda, \frac{d\lambda}{dt}, \hat{a}_t \right) &= r \cdot g \left(r, \frac{dr}{dt}, \frac{d^2r}{dt^2}, \lambda, \frac{d\lambda}{dt}, \hat{a}_t \right) / \cos \lambda = \frac{\hat{a}_t}{\cos \lambda} - 2 \frac{d\lambda}{dt} \frac{dr}{dt} - \frac{d^2r}{dt^2} \tan \lambda \\ K &= \begin{bmatrix} k_1 & k_2 \end{bmatrix} \end{aligned} \quad (24)$$

and integer $N > 0$. In the above equation,

$$a_t = n_t \cos \beta, \quad a_m = n_m \cos \lambda. \quad (25)$$

The reasons for using a high gain k are twofold. First, using a high gain instead of the derivative of the auxiliary guidance law (μ_g) allows reducing the computational complexity. Second, the high-gain loop dominates [17] the uncertain term, which comprises the time constant of the flight dynamics, and stability in the sense of Lyapunov can be guaranteed [22].

In the first step of the guidance synthesis, a control law μ_g is designed assuming idealized flight control to bound the missile-target system state trajectories. Then, in the second step, we backstep through the first-order dynamics (1) with the objective of making n_m behave as closely as possible to μ_g . In the second step, non-ideal missile dynamics are used and the target acceleration estimate is taken into account. The two-part synthesis uses the Lyapunov approach to bound trajectories of x and $(n_m - \mu_g)$.

The following subsections provide the details of the design steps. A proposition describing the trajectories of the missile-target state obtained with the proposed guidance schemes concludes the section.

3.1 Step 1: Synthesis of guidance law for idealized dynamics

Assume that flight control dynamics are ideal, i.e. $a_g = n_m = a_m / \cos \lambda$. μ_g is used as a virtual guidance law that is instrumental to the synthesis of a_g in *Step 2*. Therefore, in *Step 1* only, $\mu_g = a_g = n_m$. For brevity and for clarity of demonstration, suppose that arguments of g^* in (24) are available either as measurements or estimates. Substitution of the state-feedback guidance law (24) in (10) results in the linear system with bounded exogenous disturbance given as

$$\frac{dx}{dt} = (A + B(K + K_r))x + \frac{B}{r}(a_t - \hat{a}_t) \quad (26)$$

where A and B are given by (10), and

$$K_r = \begin{bmatrix} 0 & -\frac{Nv_{cl}}{r} \end{bmatrix}. \quad (27)$$

To determine K , the following Lyapunov function candidate is proposed

$$V(x_1, x_2) = \frac{1}{2}x^T P x \quad (28)$$

where P is a symmetric positive definite matrix and $x^T = [x_1 \quad x_2]$, x_1, x_2 are

given by (7), (8). The time-derivative of $V(x_1, x_2)$ is

$$\frac{dV}{dt}(x_1, x_2) = \frac{1}{2}x^T \left(P(A_r + BK) + (A_r^T + K^T B^T)P \right) x + x^T PB \frac{(a_t - \hat{a}_t)}{r}. \quad (29)$$

with $A_r = A + BK_r$. From *Assumption 3*, A_r is a bounded uncertain matrix. A_r can thus be expressed in a polytopic form with \underline{A}_r and \overline{A}_r representing the vertices. Since (A_r, B) forms a controllable pair, i.e. the matrix $[B, A_r B, \dots, A_r^{n-1} B]$, where n is the dimension of A_r , is non-singular, then the static state-feedback gain matrix K can be selected such that the eigenvalues of $(A_r + BK)$ are in the left-half of the complex plane if there exists a symmetric positive definite matrix Q such that

$$P(A_r + BK) + (A_r^T + K^T B^T)P = -Q \quad (30)$$

holds for $A_r \in \{\underline{A}_r, \overline{A}_r\}$ [15]. Hence, equation (29) can be written as

$$dV(x_1, x_2)/dt \leq -\frac{1}{2}x^T Qx + x^T \frac{PB}{r}(a_t - \hat{a}_t). \quad (31)$$

If the target is maneuvering with only delayed estimates $\hat{a}_t(t)$ available to the guidance law, the delay may be due to estimation computing for example, the derivative of the Lyapunov function candidate given by (29) can be bounded, using *Assumption 2(a)*, as

$$\frac{dV}{dt}(x_1, x_2) \leq -\frac{1}{2}x^T Qx + \left\| x^T PB \right\| \frac{\bar{a}_t}{r_m}. \quad (32)$$

In the present, the authors have opted for a linear matrix inequality (LMI) characterization of the robust pole placement problem. As discussed in [15] and [16], the choice of the gain matrix K such that $(A_r + BK)$ has all its eigenvalues with real parts to the left of $-h < 0$ for all $r \in]r_m; r_M[$ can be expressed as the following inequality:

$$P(A_r + BK) + (A_r^T + K^T B^T)P + 2hP < 0 \quad (33)$$

and solved for all $A_r \in \{\underline{A}_r, \overline{A}_r\}$.

Then, by replacing (30) by (33), (32) becomes

$$\frac{dV}{dt}(x_1, x_2) \leq -\lambda_m^P \cdot h \cdot \|x\|^2 + \frac{\bar{a}_t \sigma_M^P}{r_m} \|x\| \quad (34)$$

where σ_M^P and λ_m^P are the largest singular value and the smallest eigenvalue of $P > 0$, respectively, and $\|\cdot\|$ is the Euclidean norm of its argument. Letting $\theta \in]0, 1[$, then

$$\frac{dV}{dt}(x_1, x_2) \leq -(1 - \theta) \lambda_m^P h \|x\|^2 \text{ for } \|x\| > \frac{\sigma_M^P \bar{a}_t}{\theta \lambda_m^P h r_m}. \quad (35)$$

From Theorem 4.18 (pp. 168-174) in [22], the system is then uniformly ultimately bounded (see Definition 1); that is, time trajectories (x_1, x_2) enter a ball $B_1(O, b_1)$ centered at $O = (0, 0)$ and having radius b_1 given as

$$b_1 = \frac{\sigma_M^P \bar{a}_t}{\theta \lambda_m^P h r_m} \sqrt{\frac{\lambda_M^P}{\lambda_m^P}} \quad (36)$$

where λ_M^P is the largest eigenvalue of P . The ball B_1 is positively invariant [22] with respect to the closed-loop system (10) and (24). This means that once the state enters the ball, it stays there for all future time instants. The compact set B_1 to which the system trajectories (x_1, x_2) converge can be reduced by increasing h ; that is, by selecting new static feedback gains according to (33) which correspond to the eigenvalues of $(A_r + BK)$ being farther to the left of the complex plane.

3.2 Step 2: Guidance synthesis considering uncertain missile dynamics

Missile dynamics in closed-loop with autopilot are taken into account and are expressed as the first-order linear system (1), where the time constant is uncertain and possibly time-varying, although bounded. From *Step 1*, the virtual control law μ_g given by (24) stabilizes system (10), which can be written as

$$\frac{dx}{dt} = Ax + B \left(g - \frac{\mu_g \cos \lambda}{r} \right) + \frac{B \cos \lambda}{r} (\mu_g - n_m). \quad (37)$$

The new Lyapunov function candidate is taken to be

$$V(t, x_1, x_2, a_m) = \frac{1}{2} x^T P x + \frac{\tau_1 \cos \lambda}{2} (\mu_g - n_m)^2. \quad (38)$$

Due to the boundedness of τ_1 , $V(x_1, x_2, a_m)$ is bounded above and below by positive definite functions of x and $\mu_g - n_m$. The time derivative of $V(x_1, x_2, a_m)$

gives, after substitution of (1),

$$\begin{aligned}
\frac{dV}{dt}(t, x_1, x_2, a_m) &\leq -\frac{1}{2}x^T Qx + x^T \frac{PB}{r}(a_t - \hat{a}_t) + \tau_1 \cos \lambda (\mu_g - n_m) \left(\frac{d\mu_g}{dt} - \frac{dn_m}{dt} + x^T \frac{PB}{\tau_1 r} \right) \\
&\quad - \frac{1}{2} \left(\frac{d\tau_1}{dt} \cos \lambda + \tau_1 \frac{d\lambda}{dt} \sin \lambda \right) (\mu_g - n_m)^2 \\
&\leq -\frac{1}{2}x^T Qx + x^T \frac{PB}{r}(a_t - \hat{a}_t) + \cos \lambda (\mu_g - n_m) \left(\tau_1 \frac{d\mu_g}{dt} + n_m - a_g + x^T \frac{PB}{r} \right) \\
&\quad - \frac{1}{2} \left(\frac{d\tau_1}{dt} \cos \lambda + \tau_1 \frac{d\lambda}{dt} \sin \lambda \right) (\mu_g - n_m)^2
\end{aligned} \tag{39}$$

By considering the guidance law a_g (21) with high gain $k > 0$, (39) becomes

$$\begin{aligned}
\frac{dV}{dt}(t, x_1, x_2, a_m) &\leq -\frac{1}{2}x^T Qx + x^T \frac{PB}{r}(a_t - \hat{a}_t) \\
&\quad + \tau_1 \frac{d\mu_g}{dt} \cos \lambda (\mu_g - a_m) - k \cos \lambda (\mu_g - a_m)^2.
\end{aligned} \tag{40}$$

Backstepping usually makes use of signal derivatives, which can be computationally cumbersome. The high-gain design of [17] allows to simplify somewhat the procedure, although it guarantees only stability rather than asymptotic stability (see Definition 2). Guaranteeing stability of the closed-loop system allows to bound the magnitude of the state over all time instants, as given by the ball. This is a useful achievement for the engagement as we are able to bound the miss distance with our proposed nonlinear guidance law. From (40), the derivative of the virtual control law $d\mu_g/dt$ is multiplied by the bounded uncertainty τ_1 . However, the high-gain (k) design will prevent from having to compute $d\mu_g/dt$, and will also provide domination of the uncertain term $\tau_1 \cdot d\mu_g/dt$. The derivative is therefore avoided with the actual guidance law, which is particularly important in practice. It is important to point out that, in this memorandum, a characterization of ultimate boundedness rather than stability [17] is obtained. This is caused by the uncertain, although bounded, term $a_t - \hat{a}_t$, and the fact μ_g does not vanish at $(x, \mu_g - a_m) = (0, 0)$. The presence of the exogenous signal a_t , which is non-zero at $(0, 0)$ prevents $d\mu_g/dt$ from being linearly bounded by $\|x\|$, as required by the proof of Proposition 6.3 in [17]. Rather, an affine bound in $\|x\|$ is obtained in the present.

Let $\tilde{\mu} = \mu_g - a_m$. Assuming the control gain matrix K is such that (33) is satisfied, from (7), (9), (14) and (24), it is straightforward to find bounded, continuous functions m_1 and m_2 such that

$$\|\mu_g\| = \left\| \frac{a_t}{r} + m_1(r, \frac{dr}{dt}, \frac{d^2r}{dt^2})x_1 + m_2(r, \frac{dr}{dt}, \frac{d^2r}{dt^2})x_2 \right\|. \tag{41}$$

Hence,

$$\left\| \frac{d\mu_g}{dt} \right\| = \left\| \frac{1}{r} \frac{da_t}{dt} + \frac{d\mu_g}{dr} \frac{dr}{dt} + \frac{d\mu_g}{d(dr/dt)} \frac{d^2r}{dt^2} + \frac{d\mu_g}{d(d^2r/dt^2)} \frac{d^3r}{dt^3} + \frac{d\mu_g}{dx} \frac{dx}{dt} \right\|. \tag{42}$$

Following the proof of Proposition 6.3 in [17], one can construct a compact set $\Omega_R = \{(x, \tilde{\mu}) \mid V(x, \tilde{\mu}) \leq V_R\}$ where V_R is a level set defined by

$\|(x, \tilde{\mu})\| \leq R \implies V(x, \tilde{\mu}) \leq V_R$ for all $(x, \tilde{\mu}) \in \Omega$, which is a desired compact region of attraction. From *Assumption 2*, *Assumption 3* and compactness of Ω_R , there exist $c_1, c_2 > 0$ such that for all $\{x, \tilde{\mu}\} \in \Omega_R$

$$\left\| \frac{d\mu_g}{dt} \right\| \leq c_1 + c_2 \|x\| \quad (43)$$

and $k_{\Omega_R}^* \in \mathcal{R}$ such that for $k > k_{\Omega_R}^* > 0$, the dV/dt is expressed as

$$\frac{dV}{dt}(t, x_1, x_2, a_m) \leq -h\lambda_m^P \|x\|^2 + \frac{\bar{a}_t}{r_m} \|x\| \|P\| - k \|\tilde{\mu}\|^2 + c_2 \|x\| \|\tilde{\mu}\| + c_1 \|\tilde{\mu}\| \quad (44)$$

and can be made semi-negative definite for x outside a ball to be defined in the sequel. Completing the square of (44),

$$\begin{aligned} \frac{dV}{dt}(t, x_1, x_2, a_m) &\leq -\frac{h\lambda_m^P}{2} \|x\|^2 + \frac{\bar{a}_t \sigma_M^P}{r_m} \|x^T\| - \frac{h\lambda_m^P}{2} \left(\|x\| - \frac{c_2}{h\lambda_m^P} \|\tilde{\mu}\| \right)^2 \\ &\quad - \left(k - \frac{c_2^2}{2h\lambda_m^P} \right) \|\tilde{\mu}\|^2 + c_1 \|\tilde{\mu}\| \end{aligned} \quad (45)$$

$$\leq -\frac{h\lambda_m^P}{2} \|x\|^2 + \frac{\bar{a}_t \sigma_M^P}{r_m} \|x^T\| - \left(k - \frac{c_2^2}{2h\lambda_m^P} \right) \|\tilde{\mu}\|^2 + c_1 \|\tilde{\mu}\|. \quad (46)$$

Constant k is determined by a desired attraction region included in Ω_R ; that is, the given compact set Ω_R determines constants c_1 and c_2 which in turn force $k_{\Omega_R}^*$ to be greater than or equal to $\frac{c_2^2}{2h\lambda_m^P}$. Following the same rationale as in *Step 1*, consider $0 < \theta < 1$ and $0 < \kappa < 1$ such that

$$\frac{dV}{dt}(t, x_1, x_2, a_m) \leq -\frac{h\lambda_m^P}{2} (1 - \theta) \|x\|^2 - c_1 (1 - \kappa) \|\tilde{\mu}\|^2 \quad (47)$$

is valid for $\|x\| \geq \frac{2\bar{a}_t \sigma_M^P}{\lambda_m^P \theta h r_m}$ and $\|\tilde{\mu}\| \geq \frac{c_1}{\kappa} \left(k - \frac{c_2^2}{2h\lambda_m^P} \right)^{-1}$. From Theorem 4.18 (pp. 168-174) in [22], the latter development means that the system trajectory under control law (21) and (24) in $(x, \tilde{\mu})$ converges in finite time ($t_f - t_0$ is finite) to a ball centered at $(0, 0)$ and of radius b_2 given by

$$b_2 = b_2^r \sqrt{\frac{\max(\lambda_M^P, \overline{\tau_1})}{\min(\lambda_m^P, \underline{\tau_1})}} \quad (48)$$

where $b_2^r = \max \left(\frac{2\bar{a}_t \sigma_M^P}{\lambda_m^P \theta h r_m}, \frac{c_1}{\kappa} \left(k - \frac{c_2^2}{2h\lambda_m^P} \right)^{-1} \right)$. The ball is positively invariant [22] with respect to the closed-loop system (1), (10), (14), (21) and (24).

Figure 4 shows a typical state trajectory. The terminal guidance is triggered at time t_0 , whereas t_f corresponds to actual flight time. At some time instant

during the engagement, the state enters a ball of radius b_2 and stays there.

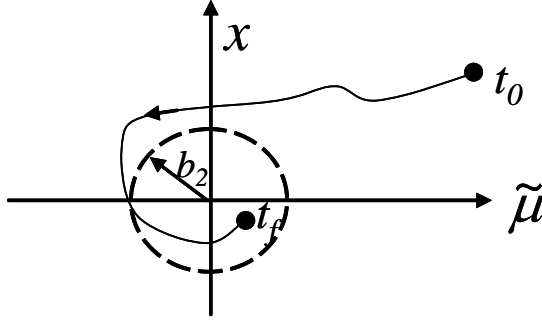


Figure 4: Missile-target trajectories

The following proposition states the qualitative property of the trajectories obtained with the nonlinear guidance.

PROPOSITION 1 Trajectories of the missile-target system given by (1), (10)-(14) in closed-loop with the nonlinear guidance law defined by state feedback (21)-(24) and solved using the LMI technique (33) are ultimately bounded with an ultimate bound b_2 given by (48). With unitary flight dynamics, trajectories of (10) in closed-loop with (24) are ultimately bounded with bound b_1 (36).

PROOF:

Proof of Proposition 1 is based on a two-step backstepping procedure described in [17] which is directly applied to the strict-feedback form system (1), (10)-(14). First, when the flight control dynamics is considered as ideal, a Lyapunov function candidate is proposed to prove the stability of (10)-(14) in closed-loop with the virtual guidance law (24). Second, with first-order flight control dynamics (1), the Lyapunov function candidate is appropriately augmented to synthesize (21) so that the stability of (21)-(24) in closed loop with the plant can be proved.

Remarks

1) In *Step 1*, if the target is not maneuvering, i.e. $a_t = 0$, then the target acceleration estimate should be set to $\hat{a}_t = 0$. From (29),

$$\frac{dV}{dt}(x_1, x_2) \leq -\frac{1}{2}x^T Qx \quad (49)$$

and asymptotic stability of the equilibrium state is guaranteed since the Lyapunov function candidate decreases on the trajectories x of system (10).

2) In *Step 1*, there exists a trade-off between the selection of a relatively small radius b_1 (36), and hence of the smallest upper bound of the final value of (x_1, x_2) , and the admissible control effort. It should be noted that a value of b_1

close to zero induces a near-zero miss distance as (x_1, x_2) approach zero. When states approach zero, the missile-target system is at or near equilibrium and LOS rate is approximately zero, which is desired with homing guidance. Ideally, the selection of b_1 should take into account the potential saturation of fin deflection, to avoid excessive acceleration demands on the missile. For instance, by selecting the eigenvalues of $(A_r + BK)$ to be far to the left of the complex plane (h is large) then b_1 is made small, and the convergence rate of the (x_1, x_2) trajectories becomes faster at the expense of possible undesirably large transient signals. Clearly, numerical simulations must be performed to determine values of K and b_1 satisfying a reasonable trade-off. Finally, it should be noted that the delay induced by the target acceleration estimate, as described in *Assumption 2(a)*, is taken into account by the nonlinear guidance law by means of the bound \bar{a}_t . However, exact zero miss distance cannot be guaranteed.

3) Radius b_2 can be decreased by tuning guidance law gain K such that h increases. The same holds true for gain k . Parameters θ and κ can also be used to decrease b_2 at the expense of a fast convergence. As noticed in (2) for *Step 1*, a trade-off exists between a small value of b_2 and an undesirable control effort.

4) When flight control dynamics are modeled as unitary, the PNG law $(N + 2) v_{cl} d\lambda/dt$ with $N > 0$ is embedded in the guidance law μ_g .

5) The implementation of the guidance law (21), (24) requires the knowledge of $r, dr/dt, d^2r/dt^2, \lambda, d\lambda/dt$ and n_m . Furthermore, estimate of the target acceleration (\hat{a}_t) is needed. If the flight path angle β of the target remains small, a_t can be considered equal to the normal acceleration n_t .

4. Numerical simulations

4.1 Numerical models and guidance laws

The proposed guidance law (21), (24), labeled as Nonlinear Proportional Navigation Guidance (NLPNG), is simulated with more realistic second-order flight control system dynamics, from commanded to actual accelerations, given as

$$\frac{a_m}{a_g} = \frac{\tau_2 s + 1}{\frac{s^2}{\omega^2} + \frac{2\xi s}{\omega} + 1} \quad (50)$$

for which the nominal parameters [23] are given by (51) and the standard deviations, based on uniform distributions, are given in (52). In (52), σ_ω is the standard deviation of the natural frequency ω , and σ_ξ is the standard deviation of the damping ratio ξ .

$$\bar{\omega} = 6.71 \text{ rad/s}, \bar{\xi} = 1.88, \tau_2 = -2.48 \cdot 10^{-2} \text{ s} \quad (51)$$

$$\sigma_\omega = 1.15 \text{ rad/s}, \sigma_\xi = 5.7 \cdot 10^{-2} \quad (52)$$

A block diagram of the missile-target model used in the numerical simulations of the terminal phase of the engagement is shown in Figure 5. The model comprises missile-target kinematics, seeker dynamics, acceleration saturation, flight control dynamics and guidance law. The terminal phase of the engagement is modeled and simulated with the Matlab software [24].

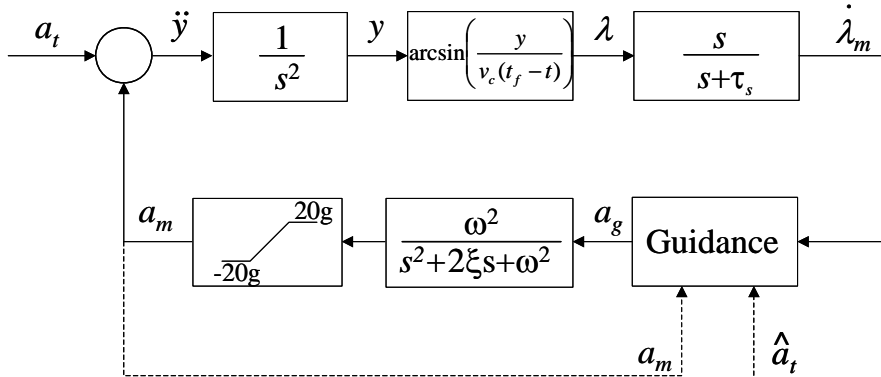


Figure 5: Block diagram of missile control system

The second-order system (50) with the numerical values of (51) has a time constant of approximately $\tau = 0.56$ s. However, the design and tuning of NLPNG (21) to (24), is based on a first-order flight control dynamics given as $a_m/a_g = 1/(\tau_1 s + 1)$. The missile-to-target range is assumed to be exactly given by $r = v_c(t_f - t)$, $v_{cl} = 1000$ m/s and $d^2r/dt^2 = 0$. The following parameters are

used in (21), (24): gain N , which is the proportional navigation constant, is selected to a large value of 5 for best PNG performance; state feedback gains, which are calculated through standard pole-placement tools such that the two poles of $A + BK$ are equal to $-0.5(1 \pm j)$, are $k_1 = 0.32$, $k_2 = -0.8$ and $k = 20$.

The matrix P satisfying (33) is calculated to be $P = \begin{bmatrix} 1.35 & 7 \cdot 10^{-4} \\ 7 \cdot 10^{-4} & 4.17 \end{bmatrix}$ and thus $x^T P B r \cong 4.27(d\lambda/dt/r)/\cos \lambda$. From (51)-(52), parameter uncertainties give a maximum time constant $\bar{\tau}_1$ of 0.9 s. $\tau_1(t)$ is assumed to be slowly time-varying, thus $k_\tau \simeq 0$. Furthermore, a_m is assumed to be available. The first-order LOS rate measurement dynamics are given as

$$[d\lambda_m/dt](s)/\lambda(s) = \frac{s}{s + \tau_s} \quad (53)$$

where λ_m is the measured LOS angle, λ is true LOS angle, and $\tau_s = 0.1$ s. Our proposed nonlinear guidance law is compared against well-known guidance laws by means of numerical simulations. The so-called neoclassical approach to the guidance synthesis, as described in [19], is given as

$$\frac{a_g(s)}{[d\lambda_m/dt](s)} = 5v_{cl} \frac{(0.2304s + 1)^2}{(0.01s + 1)^2} \quad (54)$$

where $v_{cl} = 1000$ m/s. Guidance (54) is denoted as ZMDPNG in this memorandum, the so-called zero-miss distance PNG. The optimal guidance law (OGL), described in [25], is given by

$$a_g(t) = \frac{N(\zeta)}{t_{go}^2} (y(t) + t_{go} \cdot dy/dt + 0.5\hat{a}_t(t)t_{go}^2 - a_m(t)\tau_d^2 (e^{-\zeta} + \zeta - 1)) \quad (55)$$

and

$$\begin{aligned} N(\zeta) &= \frac{6\zeta^2(e^{-\zeta} + \zeta - 1)}{2\zeta^3 - 6\zeta^2 + 6\zeta + 3 - 12\zeta e^{-\zeta} - 3e^{-2\zeta}}, \\ \hat{a}_t(t) &= a_t(t - 0.2), \quad t_{go} = t_f - t, \\ \zeta &= \frac{t_{go}}{\tau_d} \end{aligned} \quad (56)$$

where $\hat{a}_t(t)$ is a delayed estimate of the target acceleration, t_{go} is the time-to-go and $\tau_d \simeq 1.5\tau_1$ is the design time constant, which is selected to account for the lag induced by the flight control dynamics [26]. The same delayed acceleration estimate is used for the implementation of the proposed NLPNG. The proposed guidance law at the terminal phase ($v_{cl} \simeq \text{constant}$) requires measurements of $r, dr/dt, \lambda, d\lambda/dt$ and n_m , and estimation of target acceleration (\hat{a}_t). OGL guidance requires signals $y, dy/dt, a_m$ and \hat{a}_t whereas ZMDPNG needs only $d\lambda/dt$.

Before comparing the performances obtained with the proposed NLPNG, ZMDPNG and OGL, the influence of the missile dynamics on the closed-loop

behavior is determined. Here, guidance law μ_g (24) synthesized in *Step 1* is used. Note that this guidance law has been proved to stabilize the missile-target system in the case of ideal missile dynamics $\mu_g = n_m$. Head-on engagement ($y = 0$ m, $dy/dt = 0$ m/s) is considered. The guidance law μ_g is expected to deteriorate when ideal missile dynamics are replaced by more realistic, slow dynamics. As shown in Figure 6, where the guidance (24) is applied to a first-order missile with model $1/(\tau s + 1)$, the slower the missile time constant, the larger the absolute value of the miss distance. In other words, when a guidance law synthesized from idealized missile dynamics is placed in closed-loop with non-idealized missile dynamics, the performance deteriorates. Further, the loss in performance is more severe with longer time constants. The same situation was observed for PNG in [1]. The lesson learned from this simulation is that the guidance synthesis for a missile with non-ideal dynamics should include a compensation, as provided by the full law a_g (21), which is complementary to (24) and developed in *Step 2*. More on this in the next subsection.

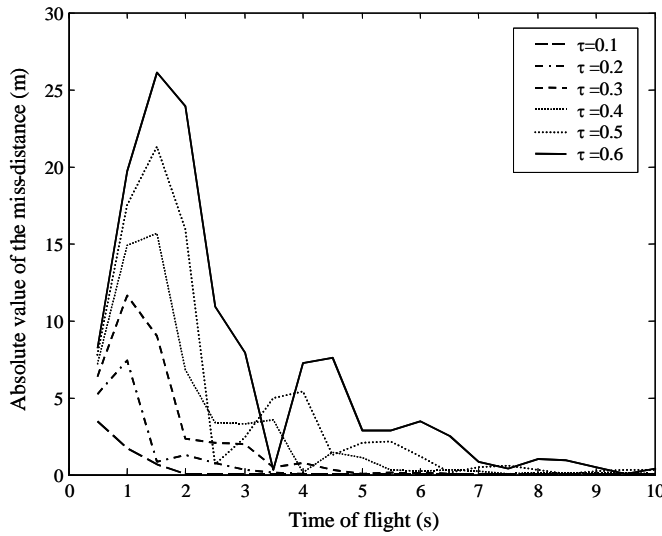


Figure 6: Influence of missile dynamics on miss distance ($a_t = 100$ m/s²)

4.2 Maneuvering target

Consider a maneuvering target with $a_t = a_t^{\max} \sin(\omega_t t)$ m/s², where $a_t^{\max} = 10g$, $g = 9.81$ m/s², $\omega_t = 1.7$ rad/s. To test the robustness of the proposed guidance law to variations in flight control dynamics, 150 simulation runs were carried out for each time of flight $t_f \in \{0.5, 1, 1.5, \dots, 10\}$ in seconds. In each simulation run, the parameters ω and ξ (51)-(52) are uniformly distributed on $[\bar{\omega} - 2, \bar{\omega} + 2]$ and $[\bar{\xi} - 0.1, \bar{\xi} + 0.1]$, respectively. Such variations in parameters are meant to represent the lack of knowledge in the true dynamic characteristics of the missile under closed-loop control and to provide a formulation of the variations in the flight envelope of the missile. It must be emphasized that if the uncertainties are

too significant, a loss in guidance performance is expected.

The impact of an acceleration estimate is determined by considering NLPNG and NLPNG + a_t , which denote the proposed guidance law with $\hat{a}_t(t) = 0$ and $\hat{a}_t(t) = a_t(t - 0.2)$, respectively. The mean values for the absolute miss distances, denoted as $E(|y(t_f)|)$, and the standard deviations for the miss distances, given as $\sigma_{y(t_f)}$, are shown in Figures 7 and 8, respectively. Miss distances obtained with classical PNG are not shown due to their prohibitively large values. Therefore, it is clear that the PNG guidance is to be avoided in situations where the target is maneuvering and missile uncertainties are present. If there is no uncertainty in the missile dynamics and autopilot, it is known that PNG may yield poor performance cite{Zarchan1}.

Figure 7 illustrates the mean value of the absolute miss distances obtained with NLPNG, NLPNG + a_t , OGL and ZMDPNG versus flight times (t_f). Guidance laws NLPNG and NLPNG + a_t give similar miss distances, which are in general smaller than those obtained with ZMDPNG and OGL. The similarities in the responses obtained with NLPNG and NLPNG + a_t come from their controller gains, which are large enough to attenuate the target acceleration, which is modelled as an exogenous disturbance in our proposed formulation. However, one advantage of NLPNG + a_t over the other techniques tested is that its controller gains are time-invariant for a given t_f , or estimated t_f . This makes the implementation of NLPNG simpler than that of OGL, making the former more appealing than the latter for real-time computations. Furthermore, NLPNG does not require an acceleration estimator. Figure 8 presents the standard deviations obtained with the various guidance laws. The proposed guidance laws provide the smallest standard deviations, except when the time of flight approaches zero. For a relatively short t_f , there is a trade-off to be made between acceptable miss distance and high gain k of the nonlinear guidance.

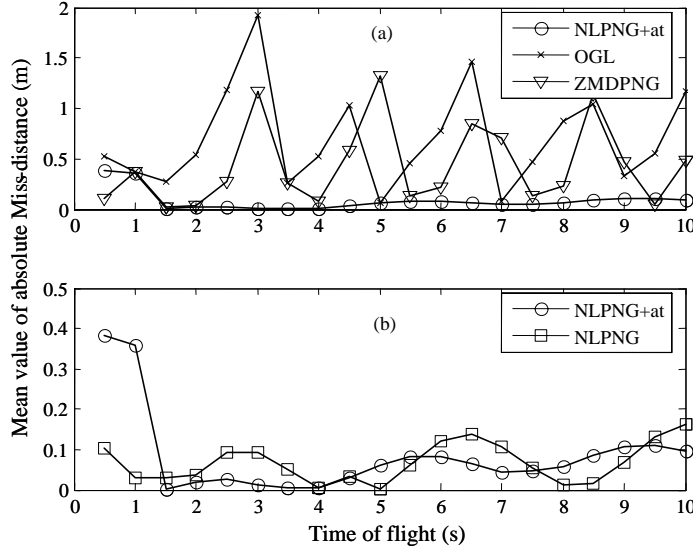


Figure 7: (a) Mean values $E(|y(t_f)|)$ for the absolute miss distances with $a_t^{\max} = 10g$, and $\omega_t = 1.7$ rad/s; (b) zoom in over $[0 \text{ m}; 0.5 \text{ m}]$

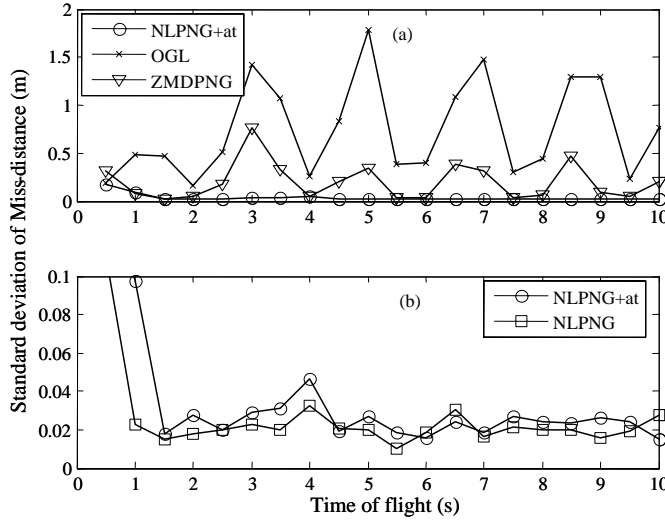


Figure 8: (a) Standard deviations $\sigma_{y(t_f)}$ on the miss distances with $a_t^{\max} = 10g$, and $\omega_t = 1.7$ rad/s; (b) zoom in over $[0 \text{ m}; 0.1 \text{ m}]$

Figure 9 presents the miss distances for different values of $\omega_t \in [0.1, 3]$ with $t_f = 5$ s and with nominal parameters $\bar{\omega}$ and $\bar{\xi}$. It is shown that the increase in miss distance obtained with the proposed guidance, as ω_t is increased, is less severe than that obtained with OGL and ZMDPNG. A lesson to be learned from the simulations is therefore that the combination of the high-gain term $k(\mu_g - n_m)$, compensating for the uncertain missile dynamics, with the

estimation of the target acceleration seems to be crucial in obtaining a relatively small miss distance, especially with a large ω_t . As seen on Figure 9, the miss distance obtained with NLPNG, the guidance law that does not use signal \hat{a}_t , becomes larger with ω_t in a manner similar to that of OGL and ZMDPNG, particularly for $\omega_t > 2.5$ rad/s.

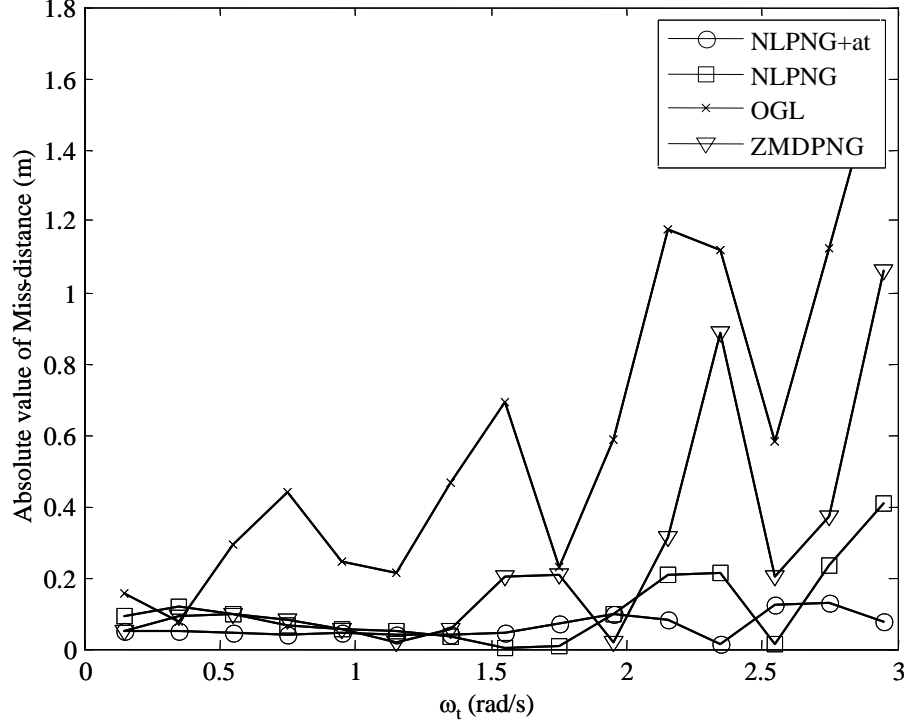


Figure 9: Absolute value of miss distance for different values of ω_t with $t_f = 5$, $a_t^{\max} = 10$ g and nominal parameters $\bar{\omega}$ and $\bar{\xi}$

Absolute values of miss distances are shown in Figure 10. There, $a_t^{\max} \in [5 \text{ g}, 10 \text{ g}]$, $t_f = 5$ s, $\omega_t = 1.7$ rad/s and nominal values are used for the parameters $\bar{\omega}$ and $\bar{\xi}$. Figure 10 suggests that using estimates of the target acceleration in the guidance law, as is the case for NLPNG+ a_t , can result in relatively small miss distances for $a_t^M \geq 12$ g; that is, for $a_m^{\max}/a_t^{\max} < 1.6$. However, performance deterioration could occur with the presence of a large delay, due to the estimation process, or from the absence of an estimate when a_t^{\max} is large. This phenomenon can be explained from the Lyapunov-based synthesis presented in this memorandum. The ultimate bound b_2 is an increasing function of \bar{a}_t , which is an upper bound on $|\hat{a}_t(t) - a_t(t)|$, from *Assumption 2*. A good estimate of $a_t(t)$ therefore leads to smaller $|\hat{a}_t(t) - a_t(t)|$ and b_2 , which is expected to result in a reduced miss distance. From Figures 9 and 10, it is clear that using a bounded $\hat{a}_t(t)$ in the nonlinear guidance robustifies the performance of the closed-loop system with respect to variations in target acceleration, which is especially important in the case of pursuer-evader maximum maneuverability ratio a_m^{\max}/a_t^{\max} [18] close to unity and large pulsation ω_t . The reader is reminded

that a maneuverability ratio close to unity indicates that target and pursuer have an acceleration of the same order of magnitude. In such a situation, the intercept is difficult to achieve. However, when a_m^{\max}/a_t^{\max} is relatively large and ω_t is small, meaning low target maneuverability, Figures 7, 9 and 10 suggest that using the bounded estimate \hat{a}_t in the guidance law is not required to improve performance.

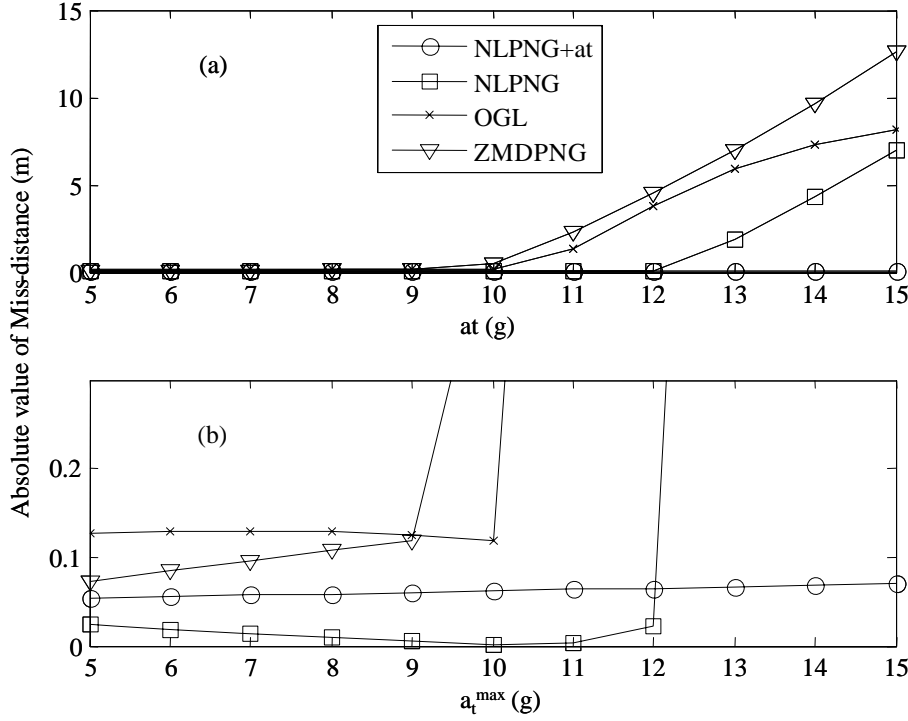


Figure 10: (a) Absolute value of miss distance for different values of a_t^{\max} (g) with $t_f = 5$, $\omega_t = 1.7$ rad/s and nominal parameters $\bar{\omega}$ and $\bar{\xi}$; (b) zoom in over $[0 \text{ m}, 3 \text{ m}]$

Figure 11 shows mean values of the energy consumed $E \left(\int_0^{t_f} a_m^2(\tau) d\tau \right)$ for the set of t_f . In the figure, the energy consumption of the proposed guidance remains slightly under that of OGL for $t_f \geq 3$ s while that of ZMDPNG is the smallest among the guidance laws tested, a performance already noticed in [19]. The higher energy consumption of NLPNG is a drawback, leading to a potential increase in drag and a reduced firing envelope when compared to ZMDPNG. It is important to point out that OGL has not been designed to take into account the parametric uncertainties and that the models used in the numerical simulations differ from those involved in OGL synthesis. Thus, sub-optimal performance is expected from OGL.

Figure 12 shows the missile accelerations for $t_f = 5$ s. The results are obtained with $\omega_t = 1.7$ rad/s and with nominal parameters $\bar{\omega}$ and $\bar{\xi}$. Accelerations obtained with NLPNG+ a_t and NLPNG saturate in the early stage of the

engagement. Saturation is, to some extent expected due to the high gains involved in the proposed guidance, especially in the early part of the terminal phase, as the proposed guidance is an asymptotic-type design with control inputs being of largest magnitude early on. Evidently, the use of high gains can undesirably amplify signal noise. However, the fact NLPNG+ a_t and NLPNG result in non-saturating accelerations near the end of the engagement could potentially allow the missile to intercept a maneuverable target by having the necessary capacity to react near the end of the engagement. Therefore, a theoretical proof of stability and performance in presence of noise and saturation could potentially be obtained by the application of advanced backstepping techniques, such as those described in [27], [28].

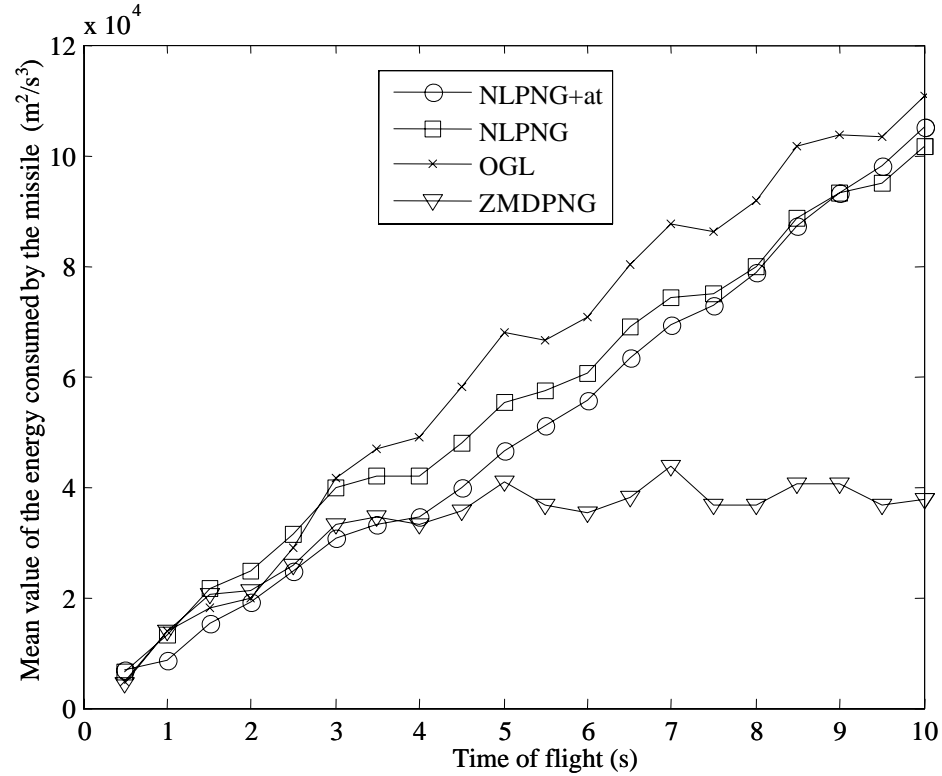


Figure 11: Mean value of the energy consumed by the missile $E\left(\int_0^t a_m^2(\tau)d\tau\right)$ with $\omega_t = 1.7$ rad/s and $a_t^{\max} = 10$ g

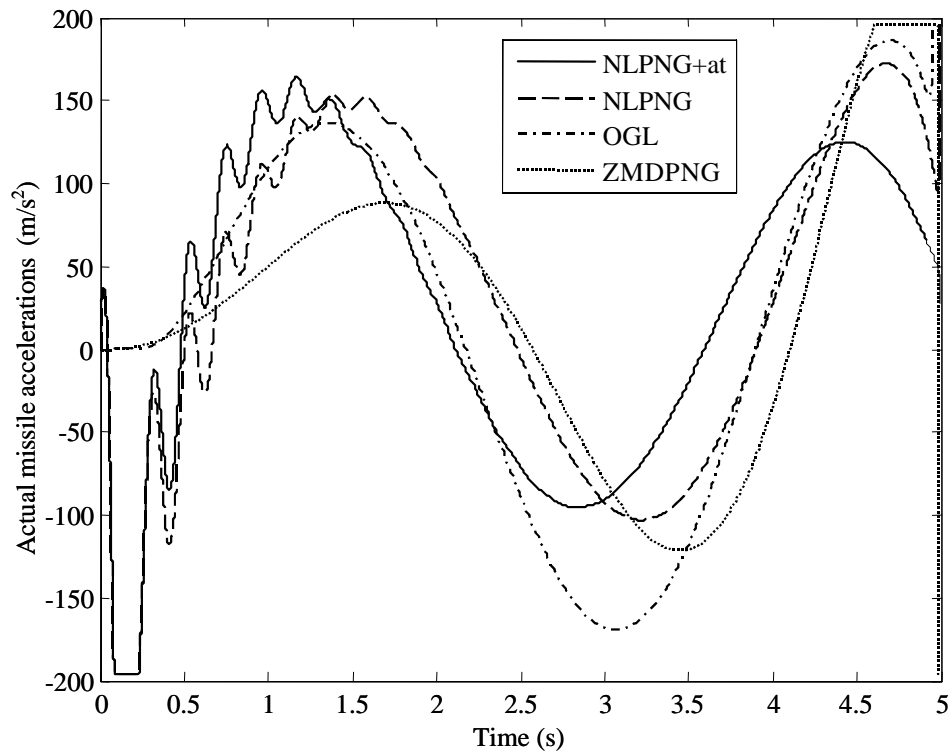


Figure 12: Comparison of actual missile accelerations with $\omega_t = 1.7$ rad/s, $a_t^{\max} = 10$ g and nominal parameters $\bar{\omega}$ and $\bar{\xi}$

5. Concluding remarks

This technical memorandum presented a nonlinear guidance law that ensures ultimate boundedness of the missile-target system trajectories when the estimate of target acceleration is uncertain, although bounded in magnitude, and the missile dynamics in closed-loop with the autopilot are uncertain. The nonlinear guidance, which takes into account the nonlinear relative kinematics between the missile and the target, is divided into two steps. In the first step, a state-feedback law is obtained from a linear matrix inequality pole characterization, assuming ideal missile dynamics in closed-loop with the autopilot; that is, a zero time constant between commanded and actual accelerations. In the second step, the guidance law is extended to take into account the uncertain dynamics by means of a high-gain backstepping approach. As described in the literature, high-gain backstepping prevents from having to compute the derivative of the virtual control law, which could amplify high-frequency noise. The nonlinear guidance law was validated by means of a numerical example which illustrated a single missile pursuing a single, maneuvering target during the terminal phase of the engagement. Terminal phase is when homing guidance, such as PNG and the proposed nonlinear guidance law, are applied. The proposed nonlinear guidance law compared advantageously with other well-known guidance laws in terms of miss distance, even in the presence of relatively slow missile dynamics. Numerical simulations showed that the proposed guidance law may require high-amplitude accelerations early on during the terminal phase, whereas no saturation is exhibited near the end of the engagement. In the future, a detailed stability analysis involving measurement noise should be carried out, an estimator of target state could be devised, and a fully nonlinear engagement model could be used in the simulations.

6. References

1. P. Zarchan, *Tactical and Strategic Missile Guidance*, American Institute of Aeronautics and Astronautics, Progress in Astronautics and Aeronautics, Volume 199, 2002.
2. Gurfil, M. Jodorkovsky and M. Guelman, Neoclassical Guidance for Homing Missiles, *Journal of Guidance, Control, and Dynamics*, Vol. 24, No. 3, 452-459, May/June 2001.
3. E. Kreindler. Optimality of proportional navigation, *AIAA Journal*, 11(6):878-880, 1973.
4. N. Lechevin, C.A. Rabbath, A. Tsourdos, B.A. White and L. Bruyere, Synthesis of Lyapunov-based Nonlinear Missile Guidance for a Class of Maneuvering Targets, *Proceedings of the IEEE Conference on Decision and Control 2004*, Paradise Island, The Bahamas, 2149-2154.
5. J. Ha and S. Chong, "Design of a CLOS Guidance Law via Feedback Linearization", *IEEE Transactions on Aerospace and Electronic Systems*, vol. 28, no. 1, 1992, pp. 51-63.
6. S. Bezick, I. Rusnack and W.S. Gray, "Guidance of a Homing Missile via Nonlinear Geometric Control Methods", *Journal of Guidance, Control and Dynamics*, Vol. 18, No. 3, pp. 441-448, May-June 1995.
7. F.-K. Yeh, K.-Y. Cheng and L.-C. Fu, "Variable Structure Based Nonlinear Missile Guidance and Autopilot Design for a Direct Hit with Thrust Vector Control", In *Proceedings of the 41st IEEE Conference on Decision and Control*, Las Vegas, Nevada, 2002, pp. 1275-1280.
8. C.-Y. Kuo, D. Soetanto and Y.-C. Chiou, "Geometric Analysis of Flight Control Command for Tactical Missile Guidance", *IEEE Transactions on Control Systems Technology*, Vol. 9, No. 2, March 2001, pp. 234-243.
9. R.T. Yanushevsky and W.J. Boord, "A New Approach to Guidance Law Design," In *AIAA Guidance, Navigation and control Conference and Exhibit*, Austin Texas, August 11-14, 2003.
10. T. L. Vincent and R.W. Morgan, "Guidance Against Maneuvering Targets Using Lyapunov Optimizing Feedback Control", In *Proceedings of the American Control Conference*, Anchorage, Alaska, 2002, pp. 215-220.
11. I.R. Manchester and A.V. Savkin, "Circular Navigation Guidance Law for Precision Missile/Target engagements", In *Proceedings of 41st IEEE Conference on Decision and Control*, Las Vegas, Nevada, 2002, pp. 1287-1292.
12. J.Z. Ben-Asher and I. Yaesh, "Advances in Missile Guidance Theory," *Progress in Astronautics and Aeronautics*, AIAA, vol. 180, 1998.

13. M. Sharma and N.D. Richards, "Adaptive, Integrated Guidance and Control for Missile Interceptors," In *AIAA Guidance, Navigation and control Conference and Exhibit*, Providence, Rhode Island, August 16-19, 2004.
14. D. Chwa and J.Y Choi, "Adaptive Nonlinear Guidance Law Considering Control Loop Dynamics," *IEEE Transactions on Aerospace and Electronic Systems*, Vol. 39. No. 4, October 2003, pp. 1134-1143.
15. M. Chilali, P. Gahinet and P. Apkarian, "Robust Pole Placement in LMI Regions," *IEEE Transactions on Automatic Control*, Vol. 44, no. 12, pp. 2257-2270, December 1999
16. M. Chilali and P. Gahinet, " H_∞ design with pole placement constraints: an LMI approach", *IEEE Transactions on Automatic Control*, Vol. 41, Vol. 3, pp.358-367, March 1996.
17. R. Sepulchre, M. Jankovic and P.V. Kokotovic, *Constructive Nonlinear Control*, Communications and Control Engineering, Springer Verlag, 1997.
18. J. Shinar and T. Shima, "Nonorthodox Guidance Law Development Approach for Intercepting Maneuvering Targets," *AIAA Journal of Guidance, Control and Dynamics*, Vol. 25, No. 4, 658-666, July-August 2002.
19. P. Gurfil, "Robust Guidance for Electro-Optical Missiles," *IEEE Transactions on Aerospace and Electronic Systems*, Vol. 39, No. 2, pp. 450-461, 2003.
20. M. G. Safonov and R. Y. Chiang. "A Schur method for balanced-truncation model reduction", *IEEE Transactions on Automatic Control*, 34:729-733, 1989.
21. P.K. Menon, G.D. Sweriduk and E.J. Ohlmeyer, "Optimal Fixed-Interval Integrated Guidance-Control Laws for Hit-to-Kill Missiles", *AIAA Guidance, Navigation and control Conference and Exhibit*, Austin Texas, August, 2003.
22. H.K. Khalil, *Nonlinear Systems*, 3rd edition, Upper Saddle River, NJ: Prentice-Hall, 2002.
23. P. Gurfil, "Zero-Miss Distance Guidance Law Based on Line-of-Sight Rate Measurement Only," *Control Engineering Practice*, Vol. 11, No. 7, pp. 819-832, 2003.
24. Getting Started with Matlab, Version 7, The Mathworks, Inc, 2005.
25. R.G. Cottrel, "Optimal intercept guidance for short range tactical missiles," *AIAA journal*, vol. 9, no. 7, pp.1414-1415, 1971.
26. H. Weiss and G. Hexner, "Modern Guidance Laws with Model Mismatch," In *Proceeding of IFAC Symposium on Missile Guidance*, Tel-Aviv, Israel, January 1998.
27. R. Freeman and L. Praly, "Integrator Backstepping for Bounded Controls and Control Rates," *IEEE Transactions on Automatic Control*, Vol. 43, No. 2, pp. 258-262, February 1998.

28. F Mazenc and S. Bowong, “Backstepping with Bounded Feedbacks for Time-Varying Systems,” *SIAM Journal on Control and Optimization*, Vol. 43, No. 3, pp. 856-871, 2004.

List of symbols/abbreviations/acronyms/initialisms

PNG	Proportional navigation guidance
LOS	Line of sight
LMI	Linear matrix inequalities
τ_1	Time constant of missile flight control system
n_m	Missile acceleration normal to LOS
a_g	Commanded acceleration for missile
a_m	Missile acceleration perpendicular to fixed x -axis
r	Range between missile and target
v_{cl}	Closing velocity
v_m	Missile speed
λ	LOS angle
n_t	Target normal acceleration
v_t	Target speed
y	Relative separation between missile and target perpendicular to fixed x -axis
$x = [x_1, x_2]^T$	State variables for missile-target kinematics
λ_0	Fixed LOS angle at equilibrium
\hat{a}_t	Estimate of target acceleration
\overline{a}_t	Bound on target acceleration
V	Lyapunov function
k	Nonlinear guidance gain
k_{vs}	Boolean used in nonlinear guidance law
μ_g	Auxiliary or virtual guidance law
P	Positive definite real matrix
N	Integer used in nonlinear guidance law
$\ \cdot\ $	Euclidean norm
B_1	Compact set to which trajectories converge
$\tilde{\mu}$	$\mu_g - a_m$
ω	Natural frequency associated with poles of second-order flight control
ξ	Damping ratio associated with poles of second-order flight control
σ_ω	Standard deviation associated with ω
σ_ξ	Standard deviation associated with ξ
NLPNG	Proposed nonlinear proportional navigation guidance law not using a_t
NLPNG+ a_t	Proposed nonlinear proportional navigation guidance law with a_t input
ZMDPNG	Zero miss distance proportional navigation guidance
OGL	Optimal guidance law
ω_t	Target pulsation
$E(\cdot)$	Mean value

Distribution List

Internal

- 1- DG
- 3- Document Library
- 1- H/PW
- 1- C.A. Rabbath (author)
- 1- N. Lechevin (NSERC Visiting Fellow and author)
- 1- M. Lauzon
- 1- E. Gagnon
- 1- R. Lestage
- 1- A. Jeffrey
- 1- P. Twardawa

External

- 1- Director Research and Development Knowledge and Information Management (pdf file)
- 1- Director Science and Technology Land
Defence Research and Development Canada
305 Rideau Street
Ottawa, Ontario
K1A 0K2
- 1- Director Science and Technology Air
Defence Research and Development Canada
305 Rideau Street
Ottawa, Ontario
K1A 0K2
- 1- Director Science and Technology Marine
Defence Research and Development Canada
305 Rideau Street
Ottawa, Ontario
K1A 0K2

UNCLASSIFIED
SECURITY CLASSIFICATION OF FORM
(Highest Classification of Title, Abstract, Keywords)

DOCUMENT CONTROL DATA		
1. ORIGINATOR (name and address) DRDC Valcartier	2. SECURITY CLASSIFICATION (Including special warning terms if applicable) UNCLASSIFIED	
3. TITLE (Its classification should be indicated by the appropriate abbreviation (S, C, R or U)) Synthesis of nonlinear guidance laws for missiles with uncertain dynamics		
4. AUTHORS (Last name, first name, middle initial. If military, show rank, e.g. Doe, Maj. John E.) C.A. Rabbath and N. Lechevin		
5. DATE OF PUBLICATION (month and year) 2007	6a. NO. OF PAGES 44	6b. NO. OF REFERENCES 27
7. DESCRIPTIVE NOTES (the category of the document, e.g. technical report, technical note or memorandum. Give the inclusive dates when a specific reporting period is covered.) Technical Memorandum		
8. SPONSORING ACTIVITY (name and address) DRDC Valcartier		
9a. PROJECT OR GRANT NO. (Please specify whether project or grant) 13ef	9b. CONTRACT NO. N/A	
10a. ORIGINATOR'S DOCUMENT NUMBER TM 2006-606	10b. OTHER DOCUMENT NOS N/A	
11. DOCUMENT AVAILABILITY (any limitations on further dissemination of the document, other than those imposed by security classification) <div style="margin-top: 10px;"><input checked="" type="checkbox"/> Unlimited distribution <input type="checkbox"/> Restricted to contractors in approved countries (specify) <input type="checkbox"/> Restricted to Canadian contractors (with need-to-know) <input type="checkbox"/> Restricted to Government (with need-to-know) <input type="checkbox"/> Restricted to Defense departments <input type="checkbox"/> Other</div>		
12. DOCUMENT ANNOUNCEMENT (any limitation to the bibliographic announcement of this document. This will normally correspond to the Document Availability (11). However, where further distribution (beyond the audience specified in 11) is possible, a wider announcement audience may be selected.) None		

UNCLASSIFIED
SECURITY CLASSIFICATION OF FORM
(Highest Classification of Title, Abstract, Keywords)

UNCLASSIFIED

SECURITY CLASSIFICATION OF FORM
(Highest Classification of Title, Abstract, Keywords)

13. **ABSTRACT** (a brief and factual summary of the document. It may also appear elsewhere in the body of the document itself. It is highly desirable that the abstract of classified documents be unclassified. Each paragraph of the abstract shall begin with an indication of the security classification of the information in the paragraph (unless the document itself is unclassified) represented as (S), (C), (R), or (U). It is not necessary to include here abstracts in both official languages unless the text is bilingual).

This technical memorandum describes a nonlinear guidance law for a single-missile, single-target engagement. The guidance relies on the concepts of Lyapunov stability and backstepping, which are constructive methods in nonlinear control theory. The design of the guidance law allows taking into account the nonlinear relative kinematics between the missile and the target, and ensuring ultimate boundedness of the missile-target system trajectories provided the estimation error of the target acceleration is bounded in magnitude. In other words, despite the nonlinear kinematics between the missile and the target, the guidance scheme is guaranteed to result in a relatively small miss distance between the missile and the target. The proposed guidance law provides successful intercept despite imprecisely known missile dynamics and errors in measurements of the target state, which are bound to occur in actual engagements. Furthermore, in cases when the target is highly maneuverable, such as with unmanned systems, the proposed guidance provides superior performance to that obtained with the classical proportional navigation guidance. There are two steps in designing the nonlinear guidance law. In the first step, using the fully nonlinear missile-target engagement kinematics, an appropriate Lyapunov function candidate is selected and a state-feedback law is obtained. Closed-loop pole placement using linear matrix inequalities provides an ultimate bound to the maximum allowable miss-distance, assuming idealized flight control dynamics; that is, infinitely fast reaction times for the missile. In the second step of the guidance law, the control law is robustified by means of a high-gain backstepping approach, taking into account the uncertain flight control dynamics as an uncertain although bounded time constant. Numerical simulations of the nonlinear guidance in closed-loop with a missile flight control system modeled as an interval second-order transfer function and a maneuvering target demonstrate satisfactory performances when compared to modern and classical guidance laws. Despite the uncertainty on the missile flight control system, which is usually the case in practice, the guidance law achieves small miss distances against highly maneuverable targets. However, it is important to note that the satisfactory performance of the nonlinear guidance comes at the expense of potentially large acceleration demands in the early part of the terminal phase of the engagement. There is a trade-off to be made between the reduction of the miss distance and the acceleration demands.

14. **KEYWORDS, DESCRIPTORS or IDENTIFIERS** (technically meaningful terms or short phrases that characterize a document and could be helpful in cataloguing the document. They should be selected so that no security classification is required. Identifiers, such as equipment model designation, trade name, military project code name, geographic location may also be included. If possible keywords should be selected from a published thesaurus, e.g. Thesaurus of Engineering and Scientific Terms (TEST) and that thesaurus-identified. If it is not possible to select indexing terms which are Unclassified, the classification of each should be indicated as with the title.)

Weapon engagement
Missile guidance
Backstepping
Lyapunov method
Nonlinear guidance

UNCLASSIFIED

SECURITY CLASSIFICATION OF FORM
(Highest Classification of Title, Abstract, Keywords)

Defence R&D Canada

Canada's Leader in Defence
and National Security
Science and Technology

R & D pour la défense Canada

Chef de file au Canada en matière
de science et de technologie pour
la défense et la sécurité nationale



WWW.drdc-rddc.gc.ca

